

Y₂O₃-stabilized ZrO₂, Ni, and graphene-added Mg by reactive mechanical grinding processing for hydrogen storage and comparison with Ni and Fe₂O₃ or MnO-added Mg

Myoung Youp Song^{a,*}, Eunho Choi^b and Young Jun Kwak^a

^aDivision of Advanced Materials Engineering, Hydrogen & Fuel Cell Research Center, Engineering Research Institute, Jeonbuk National University, 567 Baekje-daero, Deokjin-gu, Jeonju 54896, Korea

^bDepartment of Materials Engineering, Graduate School, Jeonbuk National University, 567 Baekje-daero, Deokjin-gu, Jeonju 54896, Korea

The optimum powder to ball ratio was examined, which is one of the important conditions in reactive mechanical grinding processing. Yttria (Y₂O₃)-stabilized zirconia (ZrO₂) (YSZ), Ni, and graphene were chosen as additives to enhance the hydriding and dehydriding rates of Mg. Samples with a composition of 92.5 wt% Mg + 2.5 wt% YSZ + 2.5 wt% Ni + 2.5 wt% graphene (designated as Mg-2.5YSZ-2.5Ni-2.5graphene) were prepared by grinding in hydrogen atmosphere. Mg-2.5YSZ-2.5Ni-2.5graphene had a high effective hydrogen-storage capacity of almost 7 wt% (6.85 wt%) at 623 K in 12 bar H₂ at the second cycle (n = 2). Mg-2.5YSZ-2.5Ni-2.5graphene contained Mg₂Ni phase after hydriding-dehydriding cycling. Mg-2.5YSZ-2.5Ni-2.5graphene had a larger quantity of hydrogen absorbed for 60 min, H_a (60 min), than Mg-2.5Ni-2.5graphene and Mg-2.5graphene. The addition of YSZ also increased the initial dehydriding rate and the quantity of hydrogen released for 60 min, H_d (60 min), compared with those of Mg-2.5Ni-2.5graphene. Y₂O₃-stabilized ZrO₂, Ni, and graphene-added Mg had a higher initial hydriding rate and a larger H_a (60 min) than Fe₂O₃, MnO, or Ni and Fe₂O₃-added Mg at n = 1.

Key words: Hydrogen storage, Grinding in H₂, Scanning electron microscopy (SEM), X-ray diffraction, YSZ, Ni, graphene addition.

Introduction

Magnesium (Mg) has several good properties for hydrogen storage: it has high hydrogen storage capacity (7.6 wt% based on magnesium hydride (MgH₂) weight and 8.3 wt% based on Mg weight), is relatively inexpensive, and has high reserves in the earth's crust. However, the reaction kinetics of magnesium with hydrogen is slow. The potential of magnesium hydride as a reversible hydrogen storage medium has drawn attention to improving the reaction kinetics of magnesium with hydrogen [1]. Many researchers have attempted to increase the hydrogen absorption and release rates of magnesium [2-7] by alloying with magnesium transition metals [8, 9] such as Cu, Ni, Ti, and Fe and by synthesizing compounds such as LaMg₁₂ and CeMg₁₂ [10].

Oxides can be easily pulverized during mechanical grinding since they are brittle. The added oxides and/or the oxides pulverized during mechanical grinding can make the particles of magnesium finer. The hydriding and dehydriding kinetics of Mg have also been improved

by the additions to MgH₂ or Mg of V₂O₅, VN or VC [11], Cr₂O₃ [12], Nb₂O₅ [13-16], MgO [17], Cr₂O₃, Al₂O₃ and CeO₂ [18], CeO₂ [19], and Y₂O₃ [20]. Addition of nano-sized oxides to Mg [21, 22] and coating of Ni on the Mg particles [23] are expected to improve the hydrogen-storage properties of Mg. We were interested in Yttria (Y₂O₃)-stabilized zirconia (ZrO₂) (YSZ) as an additive. Due to its hardness and chemical inertness, it is used for tooth crowns [24]; and due to its hardness and optical properties in monocrystal form, is used as jewelry. YSZ is also used as the solid electrolyte in solid oxide fuel cells (SOFCs) [24].

The addition of Ni to Mg is known to increase the hydriding and dehydriding rates of Mg [25-28]. Graphite, one of the allotropes of carbon, has high thermal conductivity compared with most metals. When graphite is added to Mg, it can thus help the sample disperse heat rapidly. The average specific gravity of graphite is 1.6-2.0, which is smaller than the specific gravity of aluminum, and the specific surface area of graphite is large. Graphene, another allotrope of carbon, has a theoretical specific surface area (SSA) of 2,630 m²/g [29]. We were also interested in Ni and graphene as additives.

One of the important conditions in reactive mechanical grinding processing is powder to ball ratio. In this work, the optimum powder to ball ratio was examined. Yttria (Y₂O₃)-stabilized zirconia (ZrO₂) (YSZ), Ni, and

*Corresponding author:
Tel : +82-63-270-2379
Fax: +82-63-270-2386
E-mail: songmy@jbnu.ac.kr

graphene were expected to increase the hydriding and dehydriding rates of Mg when added. They were thus chosen as additives. Samples with a composition of 92.5 wt% Mg + 2.5 wt% YSZ + 2.5 wt% Ni + 2.5 wt% graphene were prepared by grinding in a planetary ball mill in hydrogen atmosphere (reactive mechanical grinding). The hydriding and dehydriding properties of the prepared samples were examined. The samples were designated as Mg-2.5YSZ-2.5Ni-2.5graphene. The initial hydriding rate and the quantity of hydrogen absorbed for 60 min, H_a (60 min), of Y_2O_3 -stabilized ZrO_2 , Ni, and graphene-added Mg at the first cycle were compared with those of Fe_2O_3 , MnO, or Ni and Fe_2O_3 -added Mg.

Experimental Details

The optimum powder to ball ratio for Mg-10 Fe_2O_3 with a composition of 90 wt% Mg + 10 wt% Fe_2O_3 was examined varying the powder to ball ratios (weight ratio of powder to ball) among 1/45, 1/27, and 1/9. The average particle size of Fe_2O_3 used for this experiment was smaller than 5 μm .

The starting materials to prepare the sample Mg-2.5YSZ-2.5Ni-2.5 graphene were pure Mg powder (-20 +100 mesh, 99.8%, metals basis, Alfa Aesar), YSZ (partially-stabilized zirconia powder with uniform dispersion of 3 mol% yttria, prepared by the co-precipitation method, Tosoh, Japan), Ni (Nickel powder APS, 2.2-3.0 μm , purity 99.9% metal basis, C typically < 0.1%, Alfa Aesar), and graphene (3-10 multi-layer graphene, 5-10 μm , purity ≥ 99 wt%, thickness 3-6 nm, surface area 150 m^2/g , chemical exfoliation proprietary method, Carbon Nano-material Technology Co., Ltd).

Reactive mechanical grinding was performed in a planetary ball mill (Planetary Mono Mill; Pulverisette 6, Fritsch). Mixtures with a composition of 92.5 wt% Mg + 2.5 wt% YSZ + 2.5 wt% Ni (total weight = 7.8 g) were mixed in a stainless steel container (with 105 hardened steel balls, total weight = 360 g) that was hermetically sealed. In order to prevent oxidation, all sample handling was performed in a glove box filled with Ar. The disc revolution speed was 400 rpm. The mill container (volume of 250 ml) was then filled with high-purity hydrogen gas (≈ 12 bar). The reactive mechanical grinding was performed for 12 h, refilling the hydrogen every two hours.

To prepare Mg-2.5YSZ-2.5Ni-5graphene, the addition of graphene (0.2 g) was also performed in a planetary ball mill (Planetary Mono Mill; Pulverisette 6, Fritsch) under similar conditions to those for the preparation of 92.5 wt% Mg + 2.5 wt% YSZ + 2.5 wt% Ni for 30 min. The sample to ball weight ratio was 1/45.

The absorbed or released hydrogen quantity was measured as a function of time using a volumetric method with a Sievert's type hydriding and dehydriding apparatus that was previously described [30]. During the

measurements, the hydrogen pressures were maintained as nearly constant by replenishing the absorbed hydrogen from a small reservoir of known volume during the hydriding reaction and by removing the released hydrogen to the small reservoir during the dehydriding reaction. The 0.5 g of the samples was used for the measurement of the absorbed or released hydrogen quantity as a function of time. After the absorbed and then released hydrogen quantities were measured at 623 K for 1 h in 12 and 1.0 bar H_2 , respectively, the sample was then dehydrided at 623 K in a vacuum for 2 h.

Samples after reactive mechanical grinding and after hydriding-dehydriding cycling were characterized by X-ray diffraction (XRD) with Cu $K\alpha$ radiation, using a Rigaku D/MAX 2500 powder diffractometer. The microstructures of the powders were observed using a JSM-5900 scanning electron microscope (SEM) operated at 15 kV.

Results and Discussions

The quantity of hydrogen absorbed by the sample, H_a , and the quantity of hydrogen released by the sample, H_d , were both defined using the sample weight as a standard. H_a and H_d were expressed in the unit of wt% H. The initial hydriding rate (wt% H/min) was defined as the quantity of hydrogen charged for the first 2.5 min divided by 2.5. The initial dehydriding rate (wt% H/min) was defined as the quantity of hydrogen discharged for the first 2.5 min divided by 2.5.

The variations in the initial hydriding rate and the quantity of hydrogen absorbed for 60 min, H_a (60 min), at 593K in 12 bar H_2 with the powder to ball ratio (1/45, 1/27, and 1/9) at $n = 1$ and after activation (at $n = 2$) for Mg-10 Fe_2O_3 with a composition of 90 wt% Mg + 10 wt% Fe_2O_3 are shown in Fig. 1. The starting materials to prepare the sample Mg-10 Fe_2O_3 (at a revolution speed 250 rpm and by reactive mechanical grinding for 2 h) were pure Mg powder (particle size 50 μm) and Fe_2O_3 (< 5 μm , purity 99+%, Aldrich) [31]. At $n = 1$ and after activation (at $n = 2$), the initial hydriding rate decreased as the powder to ball ratio increased; the initial hydriding rates were the highest when the powder to ball ratio was 1/45. The initial hydriding rates after activation were higher than those at $n = 1$. At $n = 1$ and after activation (at $n = 2$), H_a (60 min) decreased as the powder to ball ratio increased; H_a (60 min)'s were the largest when the powder to ball ratio was 1/45. At the powder to ball ratio of 1/45, the H_a (60 min) after activation was smaller than that at $n = 1$. On the other hand, at the powder to ball ratio of 1/27 and 1/9, the H_a (60 min)'s after activation were larger than that at $n = 1$. The decreases in the initial hydriding rate and H_a (60 min) with the increase in the powder to ball ratio show that the milling effects got better as the powder to ball ratio increased.

From the results in Fig. 1, the powder to ball ratio of

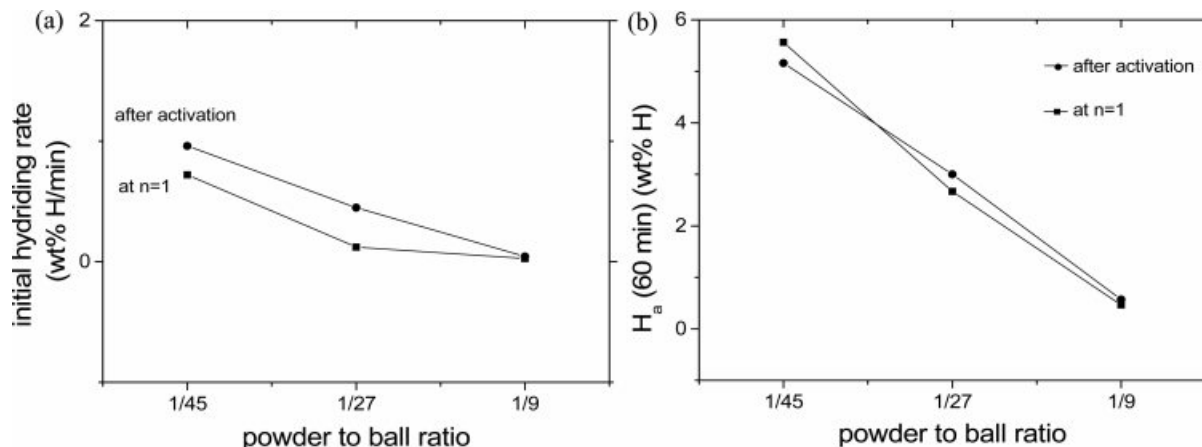


Fig. 1. Variations in (a) the initial hydriding rate and (b) the quantity of hydrogen absorbed for 60 min, H_a (60 min), at 593K in 12 bar H_2 with the powder to ball ratio at $n = 1$ and after activation (at $n = 2$) for Mg-10Fe₂O₃.

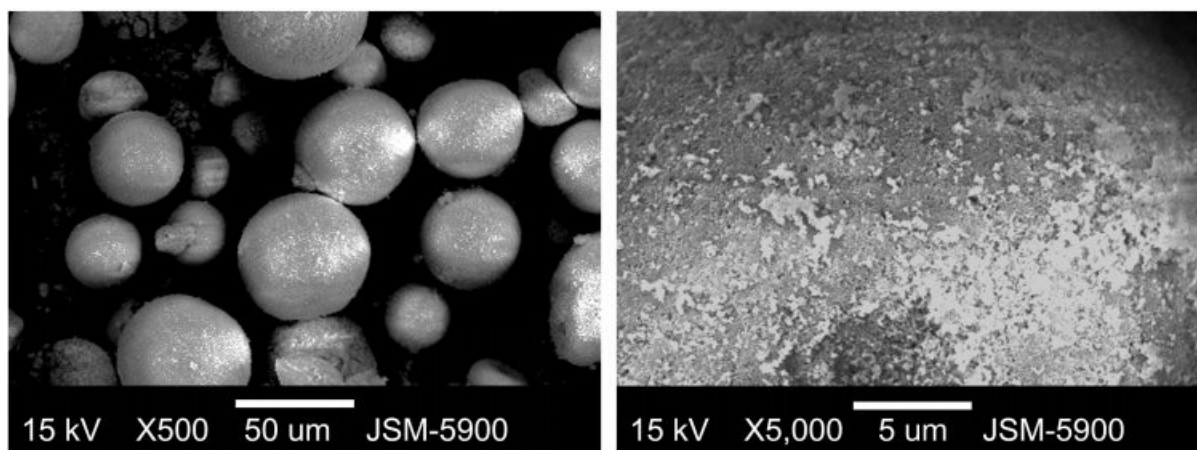


Fig. 2. SEM micrographs of YSZ at different magnifications.

1/45 was used in the process of reactive mechanical grinding for sample preparation.

The SEM micrographs of YSZ at different magnifications are shown in Fig. 2. The particles were spherical and the particle sizes were not homogeneous. The surfaces of particles were not smooth. The particles appeared to consist of fine particles, their surfaces having many defects.

Fig. 3 shows the SEM micrographs at different magnifications of Mg-2.5YSZ-2.5Ni-2.5graphene after reactive mechanical grinding and dehydrided at the 4th hydriding-dehydriding cycle. The particle sizes of the sample after reactive mechanical grinding were not homogeneous. The surfaces of the particles were smooth. The particles of this sample were much smaller than those of YSZ, indicating that the YSZ particles were pulverized during reactive mechanical grinding. The particle sizes of the sample dehydrided at the 4th hydriding-dehydriding cycle were not homogeneous, either. The particle sizes of this sample were similar to, but very slightly larger than, those of the sample after

reactive mechanical grinding. Maintenance at relatively high temperatures during hydriding-dehydriding cycling is believed to have brought about the sintering of particles and led to the very slight increase in particle size.

Fig. 4 shows the XRD pattern of Mg-2.5YSZ-2.5Ni-2.5graphene after reactive mechanical grinding. The peaks were quite broad and the background of the XRD pattern was quite high, showing that reactive mechanical grinding had led to the formation of very small crystallites. The sample contained a large amount of β -MgH₂ with small amounts of Mg, γ -MgH₂, YSZ, Ni, graphene, and MgO. β -MgH₂ and γ -MgH₂ were formed by the reaction of Mg with H_2 during grinding in hydrogen. The β -MgH₂ is a low-pressure form of magnesium hydride with tetragonal structure. The γ -MgH₂ is a high-pressure form of magnesium hydride with an orthorhombic unit cell structure of α -PbO₂ type, which usually forms in high hydrogen pressure. MgO is believed to have been formed by the reaction of Mg with oxygen adsorbed on the surfaces of as-

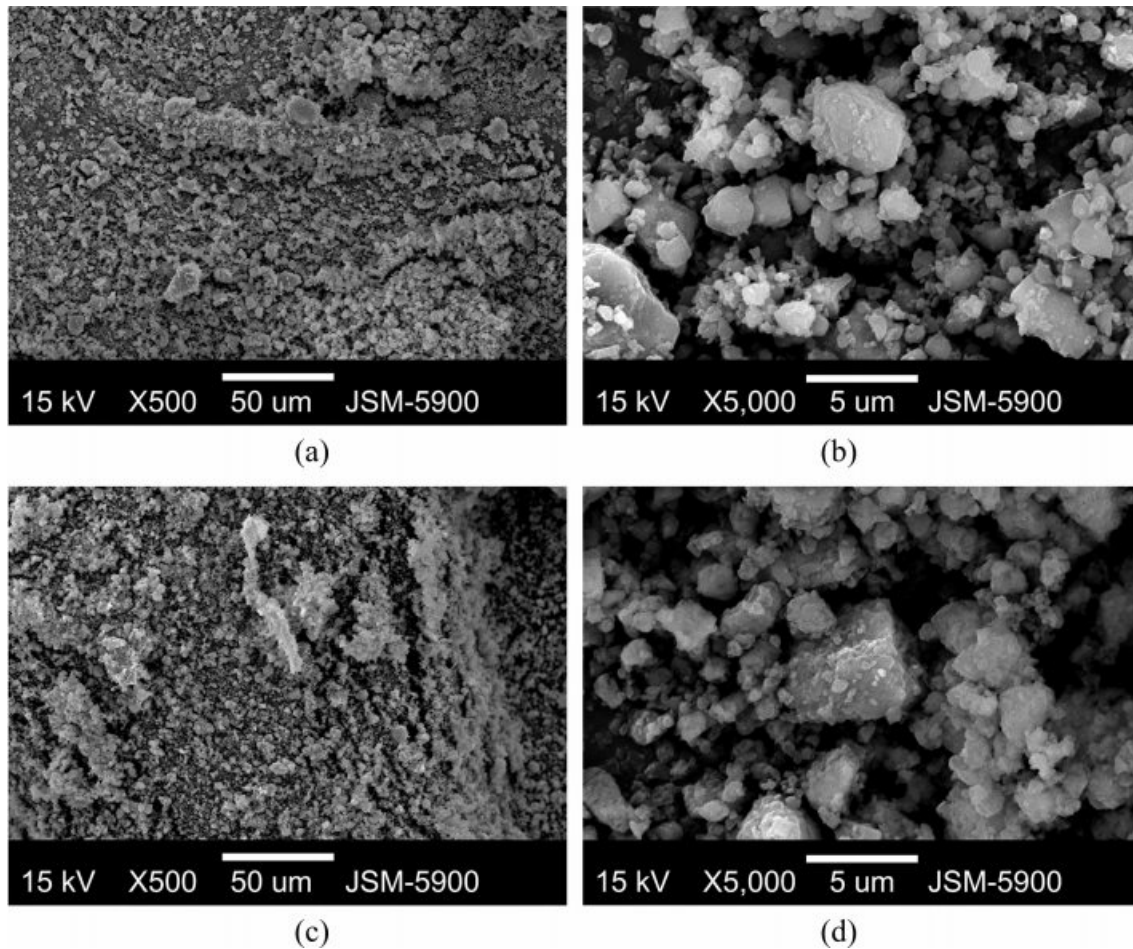


Fig. 3. SEM micrographs at different magnifications of Mg-2.5YSZ-2.5Ni-2.5graphene (a, b) after reactive mechanical grinding and (c, d) dehydrided at the 4th hydriding-dehydriding cycle.

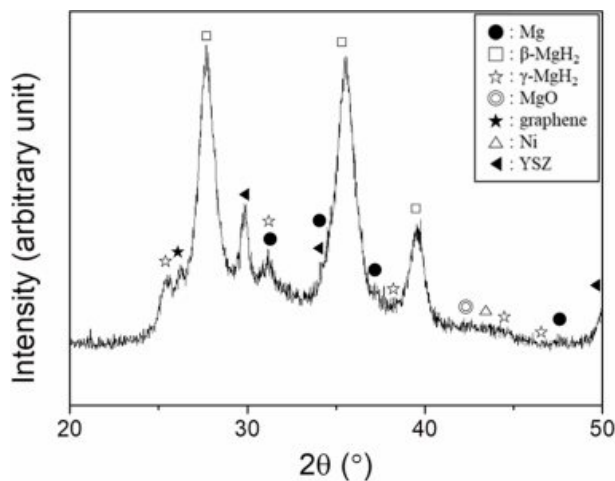


Fig. 4. XRD pattern of Mg-2.5YSZ-2.5Ni-2.5graphene after reactive mechanical grinding.

purchased Mg particles.

Table 1 presents the variations in H_a with t at 623 K in 12 bar H_2 at CN = 1-4 for Mg-2.5YSZ-2.5Ni-2.5graphene. As the number of cycles, n , increased from one to two,

Table 1. Variations in H_a with t at 623 K in 12 bar H_2 at $n = 1-4$ for Mg-2.5YSZ-2.5Ni-2.5graphene.

	2.5 min	5 min	10 min	30 min	60 min
$n = 1$	0.70	1.07	1.73	4.11	5.93
$n = 2$	2.52	3.68	5.50	6.71	6.85
$n = 3$	1.07	1.68	2.85	4.99	5.83
$n = 4$	1.87	2.75	4.10	4.99	5.18

Table 2. Variations in H_a with t at 623 K in 1.0 bar H_2 at $n = 1-4$ for Mg-2.5YSZ-2.5Ni-2.5graphene.

	2.5 min	5 min	10 min	30 min	60 min
$n = 1$	2.82	4.29	5.23	5.23	5.23
$n = 2$	2.73	4.24	5.64	5.64	5.64
$n = 3$	2.62	4.11	5.00	5.00	5.00
$n = 4$	2.69	4.22	5.03	5.05	5.05

the initial hydriding rate increased and from $n = 2$ to $n = 3$ or $n = 4$, the initial hydriding rate decreased. The quantity of hydrogen absorbed for 60 min, H_a (60 min), increased from one to two, and decreased and from $n = 2$ to $n = 4$. From $n = 1$ to $n = 2$, the increase in the initial

hydriding rate was very large. Mg-2.5YSZ-2.5Ni-2.5 graphene absorbed 1.73 wt% H for 10 min and 5.93 wt% H for 60 min at n = 1 and absorbed 5.50 wt% H for 10 min and 6.85 wt% H for 60 min at n = 2.

Table 2 presents the variations in H_d with t at 623 K in 1.0 bar H₂ at n = 1-4 for Mg-2.5YSZ-2.5Ni-2.5graphene. At n = 1, the initial dehydriding rate of Mg-2.5YSZ-2.5Ni-2.5graphene was quite high and the quantity of hydrogen released for 60 min, H_d (60 min), was quite large. As n increased from one to three, the initial dehydriding rate decreased and the initial dehydriding rate increased from n = 3 to n = 4. The quantity of hydrogen released for 60 min, H_d (60 min), increased from n = 1 to n = 2 and decreased from n = 2 to n = 3 or n = 4. Mg-2.5YSZ-2.5Ni-2.5graphene released 2.82 wt% H for 2.5 min and 5.23 wt% H for 60 min at n = 1 and released 2.73 wt% H for 2.5 min and 5.64 wt% H for 60 min at n = 2.

Table 1 and 2 show that the activation of Mg-2.5YSZ-2.5Ni-2.5graphene was completed after n = 2. An effective hydrogen storage capacity was defined as the quantity of hydrogen absorbed for 60 min. Mg-2.5YSZ-2.5Ni-2.5graphene had a high effective hydrogen-storage capacity of almost 7 wt% (6.85 wt%) at 623 K in 12 bar H₂ at n = 2.

The XRD pattern of Mg-2.5YSZ-2.5Ni-2.5graphene dehydrided at the 4th hydriding-dehydriding cycle showed that the sample contained a large amount of Mg and small amounts of MgO and β-MgH₂. Very small amounts of C, Mg₂Ni, and YSZ were also observed. MgO is believed to have been formed by the reaction of Mg with oxygen adsorbed on the surfaces of Mg particles during treatment the sample to obtain the XRD pattern. Graphene was changed to carbon after hydriding-dehydriding cycling. Mg₂Ni is believed to have been formed by the reaction of Mg with Ni. The γ-MgH₂, which was observed after reactive mechanical grinding, is believed to have been transformed to β-MgH₂ during hydriding-dehydriding cycling. The peaks in the XRD pattern were sharp and the background of the XRD pattern was very high, showing that the sample was well crystallized. The sample, which was quite amorphous after reactive mechanical grinding, became crystalline.

Fig. 5 shows the H_a vs. t curves at 623 K in 12 bar H₂ and the H_d vs. t curves at 623 K in 1.0 bar H₂ at n = 1 of a 95 wt% Mg + 5 wt% graphene alloy (named Mg-5graphene), a 95 wt% Mg + 2.5 wt% Ni + 2.5 wt% graphene alloy (named Mg-2.5Ni-2.5graphene), and Mg-2.5YSZ-2.5Ni-2.5graphene. Mg-5graphene and Mg-

2.5Ni-2.5graphene were prepared under similar conditions to those for preparing Mg-2.5YSZ-2.5Ni-2.5graphene. Mg-5graphene had the highest initial hydriding rate, followed in order by Mg-2.5YSZ-2.5Ni-2.5graphene and Mg-2.5Ni-2.5graphene. Mg-2.5YSZ-2.5Ni-2.5graphene had the largest H_a (60 min), followed in order by Mg-5graphene and Mg-2.5Ni-2.5graphene. Mg-2.5YSZ-2.5Ni-2.5graphene absorbed 1.73 wt% H for 10 min and 5.93 wt% H for 60 min. Mg-5graphene absorbed 2.67 wt% H for 10 min and 5.62 wt% H for 60 min. Table 3 presents the variations in H_a with t at 623 K in 12 bar H₂ at n = 1 for Mg-5graphene, Mg-2.5Ni-2.5 graphene, and Mg-2.5YSZ-2.5Ni-2.5graphene. Mg-2.5YSZ-2.5Ni-2.5graphene dehydrided at the 4th hydriding-dehydriding cycle contained Mg₂Ni phase. Mg-2.5Ni-

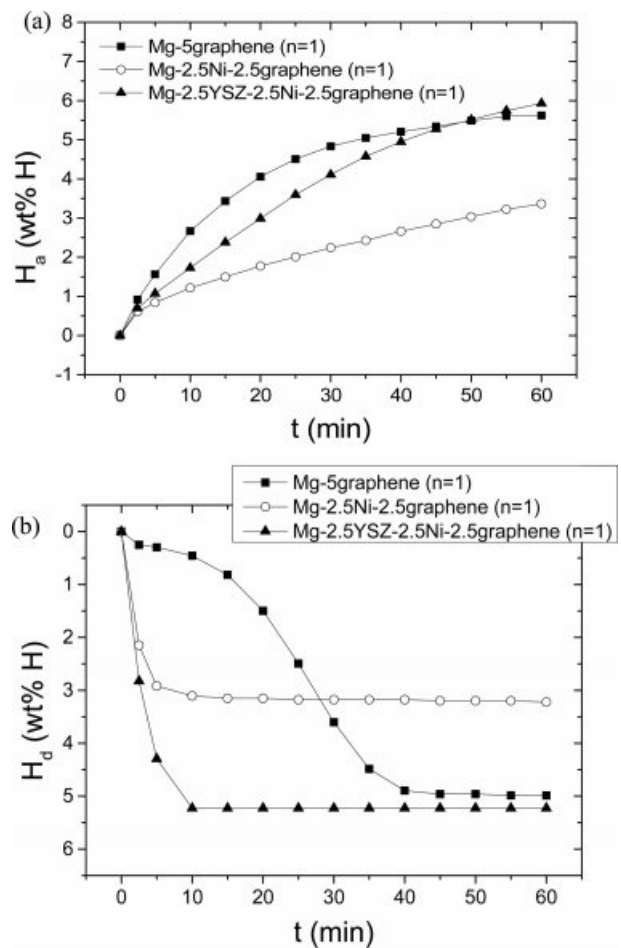


Fig. 5. (a) H_a vs. t curves at 623 K in 12 bar H₂ and (b) H_d vs. t curves at 623 K in 1.0 bar H₂ at n = 1 for Mg-5graphene, Mg-2.5Ni-2.5graphene, and Mg-2.5YSZ-2.5Ni-2.5graphene.

Table 3. Variations in H_a with t at 623 K in 12 bar H₂ at n = 1 for Mg-5graphene, Mg-2.5Ni-2.5graphene, and Mg-2.5YSZ-2.5Ni-2.5graphene.

	2.5 min	5 min	10 min	30 min	60 min
Mg-2.5YSZ-2.5Ni-2.5graphene	0.70	1.07	1.73	4.11	5.93
Mg-2.5Ni-2.5graphene	0.61	0.84	1.21	2.24	3.36
Mg-5graphene	0.92	1.57	2.67	4.83	5.62

2.5graphene after hydriding-dehydriding cycling also contained the Mg_2Ni phase. Mg_2Ni is known to have higher hydriding and dehydriding rates than Mg. The equilibrium plateau pressures at 623 K of the Mg-H and Mg_2Ni -H systems are 5.90 bar and 9.24 bar, respectively [31, 32]. At 623 K in 12 bar H_2 , the driving forces for the hydriding reaction of Mg and Mg_2Ni , which are related to the difference between the applied hydrogen pressure (12 bar H_2 in this work) and the equilibrium plateau pressure, were 6.10 bar and 2.76 bar, respectively. The slow nucleation of Mg_2NiH_4 in Mg-2.5YSZ-2.5Ni-2.5graphene and Mg-2.5Ni-2.5graphene due to the small driving force is believed to have led to the lower initial hydriding rates of Mg-2.5YSZ-2.5Ni-2.5graphene and Mg-2.5Ni-2.5graphene than that of Mg-5graphene. Mg-2.5YSZ-2.5Ni-2.5graphene had a higher initial hydriding rate than Mg-2.5Ni-2.5graphene, suggesting that the addition of YSZ increased the initial hydriding rate. After a relatively long time, for example, after 60 min, the quantity of hydrogen absorbed by Mg-2.5YSZ-2.5Ni-2.5graphene was larger than those by Mg-5graphene and Mg-2.5Ni-2.5graphene. Mg-5graphene released a small amount of hydrogen in the beginning (for 2.5 min) and then released hydrogen very slowly. Thereafter, the dehydriding rate of Mg-5graphene increased slowly, reaching its maximum after about 25 min, and was very low after 40 min. The H_d vs. t curve for Mg-5graphene exhibited an S-shaped curve, showing that the dehydriding reaction of Mg-5graphene progressed by the nucleation and growth mechanism. Mg-2.5YSZ-2.5Ni-2.5graphene had the highest initial dehydriding rate, followed in order by Mg-2.5Ni-2.5graphene and Mg-5graphene. Mg-2.5YSZ-2.5Ni-2.5graphene had the largest H_d (60 min), followed in order by Mg-5graphene and Mg-2.5Ni-2.5graphene. At 623 K in 1.0 bar H_2 , the driving forces for the dehydriding reaction of Mg and Mg_2Ni , which are related to the difference between the equilibrium plateau pressures and the applied hydrogen pressure (1.0 bar H_2 in this work), were 4.90 bar and 8.24 bar, respectively. The rapid nucleation of the Mg_2Ni -H solid solution in Mg-2.5Ni-2.5graphene and Mg-2.5YSZ-2.5Ni-2.5graphene due to the large driving force is believed to have led to the higher initial dehydriding rates of Mg-2.5Ni-2.5graphene and Mg-2.5YSZ-2.5Ni-2.5graphene than that of Mg-2.5graphene. The addition of YSZ also increased the initial dehydriding rate and H_d (60 min), compared with those of Mg-2.5Ni-2.5graphene.

Fig. 6 shows the H_a vs. time t curves at 593 K in 12 bar H_2 at $n = 1$ for pure Mg (named Mg) [33], a 90 wt% Mg + 10 wt% MnO alloy (named Mg-10MnO) [34], a 90 wt% Mg + 10 wt% Fe_2O_3 alloy (named Mg-10 Fe_2O_3) [35], 90 wt% Mg + 5 wt% Fe_2O_3 + 5 wt% Ni (named Mg-5 Fe_2O_3 -5Ni) [35], and Mg-2.5YSZ-2.5Ni-2.5graphene. The starting materials to prepare the sample Mg-10MnO (at a revolution speed 250 rpm and by reactive mechanical grinding for 2 h) were Mg powder (particle size 50 μm) and MnO (88-250 μm , purity 99%, Aldrich) [34]. The starting materials to prepare the samples Mg-10 Fe_2O_3 and Mg-5 Fe_2O_3 -5Ni (at a revolution speed 250 rpm and by reactive mechanical grinding for 2 h) were Mg (assay $\geq 99\%$, grit; 50-150 mesh, Fluka), Fe_2O_3 (nano-sized Fe_2O_3 , prepared by spray conversion process, about 36 nm), and Ni (purity 99.9%, average $\sim 5 \mu m$, CERAC) [35]. The Mg, Mg-10MnO, Mg-10 Fe_2O_3 , and Mg-5 Fe_2O_3 -5Ni samples were prepared under similar conditions to those for preparing Mg-2.5YSZ-2.5Ni-2.5graphene. The Mg absorbed hydrogen very slowly. Mg-2.5YSZ-2.5Ni-2.5graphene had the highest initial hydriding rate, followed in order by Mg-10MnO, Mg-5 Fe_2O_3 -5Ni, Mg-10 Fe_2O_3 , and Mg. Mg-2.5YSZ-2.5Ni-2.5graphene had the largest H_a (60 min), followed in order by Mg-5 Fe_2O_3 -5Ni, Mg-10MnO, Mg-10 Fe_2O_3 , and Mg. Mg absorbed 0.04 wt% H for 2.5 min, and 0.45 wt% H for 60 min [35]. Mg-2.5YSZ-

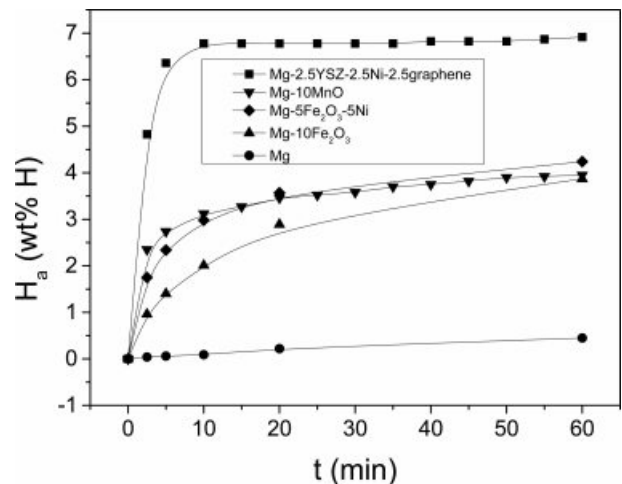


Fig. 6. H_a vs. t curves at 593 K in 12 bar H_2 at $n = 1$ for Mg [33], Mg-10MnO [34], Mg-10 Fe_2O_3 [35], Mg-5 Fe_2O_3 -5Ni [35], and Mg-2.5YSZ-2.5Ni-2.5graphene.

Table 4. Variations in absorbed hydrogen quantity (wt% H) with time at 593 K in 12 bar H_2 at $n = 1$ for Mg, Mg-10MnO, Mg-10 Fe_2O_3 , Mg-5 Fe_2O_3 -5Ni, and Mg-2.5YSZ-2.5Ni-2.5graphene.

	2.5 min	5 min	10 min	20 min	30 min	60 min
Mg	0.04	0.06	0.09	0.22	-	0.45
Mg-10MnO	2.35	2.74	3.12	3.35	3.58	3.95
Mg-10 Fe_2O_3	0.96	1.40	2.01	2.89	-	3.87
Mg-5 Fe_2O_3 -5Ni	1.75	2.34	2.98	3.57	-	4.24
Mg-2.5YSZ-2.5Ni-2.5graphene	4.83	6.36	6.78	6.78	6.78	6.92

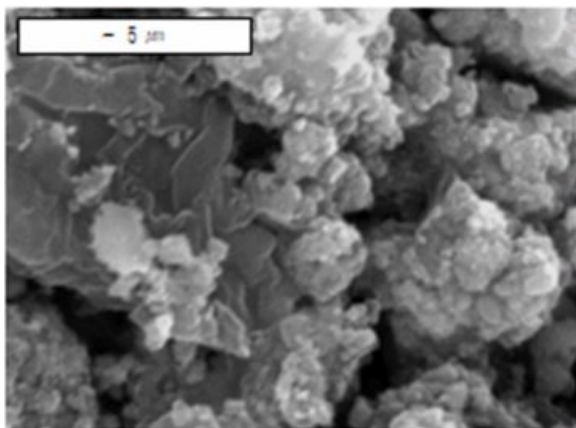


Fig. 7. A SEM micrograph of Mg-10Fe₂O₃ hydrided at the 12th hydriding-dehydriding cycle [35].

2.5Ni-2.5graphene absorbed 4.83 wt% H for 2.5 min and 6.92 wt% H for 60 min. On the other hand, Mg-10Fe₂O₃ absorbed 0.96 wt% H for 2.5 min and 3.87 wt% H for 60 min [35]. Table 4 summarizes the variations in absorbed hydrogen quantity (wt% H) with time at 593 K in 12 bar H₂ at n = 1 for these samples [33-35]. The considerably higher initial hydriding rate and considerably larger H_a (60 min) of Mg-2.5YSZ-2.5Ni-2.5graphene than Mg show that the addition of YSZ, Ni, and graphene significantly increased the initial hydriding rate and H_a (60 min).

A SEM micrograph of Mg-10Fe₂O₃ hydrided at the 12th hydriding-dehydriding cycle [35] is shown in Fig. 7. The particles of this sample were larger than those of Mg-2.5YSZ-2.5Ni-2.5graphene dehydrided at the 4th hydriding-dehydriding cycle, supporting well that the activated Mg-2.5YSZ-2.5Ni-2.5graphene had a much higher initial hydriding rate and much larger H_a (60 min) than the activated Mg-10Fe₂O₃.

The reactive mechanical grinding of Mg with YSZ, Ni, and graphene is believed to have created defects (leading to facilitation of nucleation), produced cracks and clean surfaces (leading to increase in reactivity), and decreased particle sizes (leading to diminution of diffusion distances or increasing the flux of the diffusing hydrogen atoms) [36-43].

Conclusions

The optimum powder to ball ratio for Mg-10 Fe₂O₃ was 1/45, which is one of the important conditions in reactive mechanical grinding processing. Samples with a composition of 92.5 wt% Mg + 2.5 wt% YSZ + 2.5 wt% Ni + 2.5 wt% graphene (designated as Mg-2.5YSZ-2.5Ni-2.5graphene) were prepared by grinding in hydrogen. Mg-2.5YSZ-2.5Ni-2.5graphene was completely activated after n = 2, having an effective hydrogen-storage capacity (the quantity of hydrogen absorbed for 60 min) of almost 7 wt% (6.85 wt%) at 623 K in 12

bar H₂ at n = 2. The sample absorbed 5.50 wt% H for 10 min and 6.85 wt% H for 60 min in 12 bar H₂ and released 2.73 wt% H for 2.5 min and 5.64 wt% H for 60 min in 1.0 bar H₂, at 623 K at n = 2. Mg-2.5YSZ-2.5Ni-2.5graphene contained Mg₂Ni phase after hydriding-dehydriding cycling. The slow nucleation of Mg₂NiH₄ in Mg-2.5YSZ-2.5Ni-2.5graphene and Mg-2.5Ni-2.5graphene due to the small driving force is believed to have led to the lower initial hydriding rates than that of Mg-5graphene. Mg-2.5YSZ-2.5Ni-2.5graphene had a higher initial hydriding rate than Mg-2.5Ni-2.5graphene, suggesting that the addition of YSZ increased the initial hydriding rate. Mg-2.5YSZ-2.5Ni-2.5graphene had a larger H_a (60 min) than Mg-2.5Ni-2.5graphene and Mg-2.5graphene. The rapid nucleation of Mg₂Ni-H solid solution in Mg-2.5Ni-2.5graphene and Mg-2.5YSZ-2.5Ni-2.5graphene due to the large driving force is believed to have led to their higher initial dehydriding rates than that of Mg-2.5graphene. The addition of YSZ also increased the initial dehydriding rate and the H_d (60 min), compared with those of Mg-2.5Ni-2.5graphene. Y₂O₃-stabilized ZrO₂, Ni, and graphene-added Mg had a higher initial hydriding rate and larger H_a (60 min) than Fe₂O₃, MnO, or Ni and Fe₂O₃-added Mg at the first cycle.

Acknowledgements

This research was supported by Basic Science Research Program through the National Research Foundation of Korea (NRF) funded by the Ministry of Education (grant number NRF-2017R1D1A1B03030515). This paper was supported by the selection of research-oriented professor of Jeonbuk National University in 2019.

References

1. M.Y. Song, Y.J. Kwak, S.H. Lee, and H.R. Park, *Korean J. Met. Mater.* 51[2] (2013) 119-123.
2. Y. Wang, K. Luo, W. Ye, S. Du, J.S. Francisco, J. Yin, and P. Gao, *Int. J. Hydrogen Energy* 44[29] (2019) 15239-15245.
3. S. Niyomsoan, D.R. Leiva, R.A. Silva, L.F. Chanchetti, R.N. Shahid, S. Scudino, P. Gargarella, and W.J. Botta, *Int. J. Hydrogen Energy* 44[29] (2019) 23257-23266.
4. M.Y. Song, E. Choi, and Y.J. Kwak, *Int. J. Hydrogen Energy* 44[29] (2019) 3779-3789.
5. Y.J. Kwak, S.H. Lee, and M.Y. Song, *J. Nanosci. Nanotech.* 18[9] (2018) 6040-6046.
6. M.Y. Song, E. Choi, and Y.J. Kwak, *Mater. Res. Bull.* 108 (2018) 23-31.
7. Y.J. Kwak, E. Choi, and M.Y. Song, *Met. Mater. Int.* 24[5] (2018) 1181-1190.
8. S.H. Hong, S.N. Kwon, and M.Y. Song, *Korean J. Met. Mater.* 49[4] (2011) 298-303.
9. J.J. Reilly and R.H. Wiswall Jr, *Inorg. Chem.* 7[11] (1968) 2254-2256.
10. J.M. Boulet and N. Gerard, *J. Less-Common Met.* 89 (1983) 151-161.

11. W. Oelerich, T. Klassen, and R. Bormann, *J. Alloys Compd.* 322 (2001) L5-9.
12. Z. Dehouche, T. Klassen, W. Oelerich, J. Goyette, T.K. Bose, and R. Schulz, *J. Alloys Compd.* 347 (2002) 319-323.
13. G. Barkhordarian, T. Klassen, and R. Bormann, *Scripta Materialia* 49 (2003) 213-217.
14. G. Barkhordarian, T. Klassen, and R. Bormann, *J. Alloys Compd.* 407[1-2] (2006) 249-255.
15. O. Friedrichs, T. Klassen, J.C. Sánchez-López, R. Bormann, and A. Fernández, *Scripta Materialia* 54[7] (2006) 1293-1297.
16. O. Friedrichs, F. Aguey-Zinsou, J.R. Ares Fernández, J.C. Sánchez-López, A. Justo, T. Klassen, R. Bormann, and A. Fernández, *Acta Materialia* 54[1] (2006) 105-110.
17. K.F. Aguey-Zinsou, J.R. Ares Fernandez, T. Klassen, and R. Bormann, *Mat. Res. Bull.* 41[6] (2006) 1118-1126.
18. M.Y. Song, J.-L. Bobet, and B. Darriet, *J. Alloys Compd.* 340 (2002) 256-262.
19. S. Long, J. Zou, Y. Liu, X. Zeng, and W. Ding, *J. Alloys Compd.* 580 (Supplement 1) (2013) S167-170.
20. S. Long, J. Zou, Xi Chen, X. Zeng, and W. Ding, *J. Alloys Compd.* 615 (Supplement 1) (2014) S684-688.
21. J.-I. Song, G.-Y. Lee, J.-R. Kim, and J.-S. Lee, *J. Cer. Proc. Res.* 19[4] (2018) 279-284.
22. C.W. Park, J.H. Lee, S.H. Kang, J.H. Park, H.M. Kim, H.S. Kang, H.A. Lee, J.H. Lee, J.H. In, and K.B. Shim, *J. Cer. Proc. Res.* 19[2] (2018) 179-182.
23. S.-M. Sim, *J. Cer. Proc. Res.* 19[1] (2018) 1-4.
24. https://en.wikipedia.org/wiki/Yttria-stabilized_zirconia
25. S.-H. Hong and M.Y. Song, *Korean J. Met. Mater.* 54[2] (2016) 125-131.
26. M.Y. Song, Y.J. Kwak, S.H. Lee, and H.R. Park, *Korean J. Met. Mater.* 54[3] (2016) 210-216.
27. M.Y. Song, Y.J. Kwak, and H.R. Park, *Korean J. Met. Mater.* 54[7] (2016) 503-509.
28. S.N. Kwon, H.R. Park, and M.Y. Song, *Korean J. Met. Mater.* 54[7] (2016) 510-519.
29. <https://en.wikipedia.org/wiki/Graphene>
30. M.Y. Song, S.H. Baek, J.-L. Bobet, and S.H. Hong, *Int. J. Hydrogen Energy* 35 (2010) 10366-10372.
31. M.Y. Song and Y.J. Kwak, *Korean J. Met. Mater.* 56[3] (2018) 244-251.
32. M.Y. Song and H.R. Park, *J. Alloys Compd.* 270 (1998) 164-167.
33. M.Y. Song, Y.J. Kwak, S.H. Lee, and H.R. Park, *Bull. Mater. Sci.* 37[4] (2014) 831-835.
34. M.Y. Song, I.H. Kwon, S.N. Kwon, C.G. Park, S.H. Hong, J.S. Bae, and D.R. Mumm, *J. Alloys Compd.* 415 (2006) 266-270.
35. S.N. Kwon, Improvement of the hydrogen absorption and desorption kinetics of Mg by catalytic effects of Fe₂O₃ and Ni, M.E. thesis, Jeonbuk National University, February 22, 2008.
36. M.Y. Song, S.H. Lee, and D.R. Mumm, *J. Cer. Proc. Res.* 19[3] (2018) 211-217.
37. M.Y. Song, Y.J. Kwak, and S.H. Lee, *J. Cer. Proc. Res.* 20[2] (2019) 173-181.
38. S.-H. Hong and M.Y. Song, *Korean J. Met. Mater.* 56[2] (2018) 155-162.
39. M.Y. Song, E. Choi, and Y.J. Kwak, *Korean J. Met. Mater.* 56[5] (2018) 392-399.
40. M.Y. Song, Y.J. Kwak, and E. Choi, *Korean J. Met. Mater.* 56[7] (2018) 524-531.
41. M.Y. Song and Y.J. Kwak, *Korean J. Met. Mater.* 56[8] (2018) 611-619.
42. M.Y. Song, E. Choi, and Y.J. Kwak, *Korean J. Met. Mater.* 56[8] (2018) 620-627.
43. M.Y. Song and Y.J. Kwak, *Korean J. Met. Mater.* 56[12] (2018) 878-884.